Changing Stations in Single Bistable Rotaxane Molecules under Electrochemical Control

Tao Ye,[†,‡] Ajeet S. Kumar,[†] Sourav Saha,[§,†] Tomohide Takami,[†,⊥] Tony J. Huang,[¶] J. Fraser Stoddart,[§,*] and Paul S. Weiss[†,#,*]

[†]Departments of Chemistry and Physics, The Pennsylvania State University, University Park, Pennsylvania 16802, [‡]School of Natural Sciences, University of California, Merced, 5200 N. Lake Road, Merced, California 95343, [§]Department of Chemistry, Northwestern University, Evanston, Illinois 60208, [⊥]VRI, Inc., Tokyo 150-0001, Japan, [¶]Department of Engineering Science and Mechanics, The Pennsylvania State University, University Park, Pennsylvania 16802, and [#]California NanoSystems Institute and Department of Chemistry and Biochemistry, University of California, Los Angeles, Los Angeles, California 90095. [†]Present Address: Department of Chemistry and Biochemistry, Florida State University, Tallahassee, Florida 32306.

ABSTRACT We have directly observed electrochemically driven single-molecule station changes within bistable rotaxane molecules anchored laterally on gold surfaces. These observations were achieved by employing molecular designs that significantly reduced the mobility and enhanced the assembly of molecules in orientations conducive to direct measurement using scanning tunneling microscopy. The results reveal molecular-level details of the station changes of surface-bound bistable rotaxane molecules, correlated with their different redox states. The mechanical motions within these mechanically interlocked molecules are influenced by their interactions with the surface and with neighboring molecules, as well as by the conformations of the dumbbell component.

KEYWORDS: bistable rotaxanes · electrochemistry · scanning tunneling microscopy · single-molecule motion · mechanically interlocked molecules

Mechanically interlocked molecules, such as bistable catenanes and rotaxanes having addressable rings,[1−7] have potential applications in areas ranging from molecular-scale electronics[8] to display technologies[9] to nanoelectromechanical devices.[10,11] Functional components of these molecular machines can be triggered by external stimuli, such as redox reactions,[12] light,[13] metal ion complexation,[14] and pH.[15] Solution-phase measurements have been used to characterize the structures and functions[3] of these molecular switches. However, to realize the full potential of these functional molecules at the nanoscale, it is imperative to understand their operation at the single-molecule level under environments relevant to actual device operation.[8,9,11] Recently, progress has been made in measuring collections of molecules in condensed monolayers and polymer gel matrices.[16,17] Few examples illustrate scanning tunneling microscope (STM) tip manipulation of rotaxane molecules on substrates.[18,19] However, serial manipulation of switchable molecules does not correlate directly with the structural changes of single molecules under parallel electrochemical, optical, and chemical control, which are more prevalent in nanoscale devices under development.[10]

Thus far, most rotaxane molecules are inherently flexible and have poorly defined conformations and orientations when attached to surfaces, rendering them difficult to resolve individually with scanning probe microscopes. Because of the limited knowledge of the molecular geometries and conformations of such single molecules on substrates, the effects of the nanoscale environments on the station changes remain unaddressed. In this work, we have developed molecular designs that reduce the mobilities of the molecules significantly. We were able to assemble bistable rotaxane molecules in orientations conducive to direct STM measurements of their station changes. Electrochemical scanning tunneling microscopy (ECSTM) has been employed to observe molecular motion *in situ*,[20,21] and we observed that single-molecule station changes correlate with the redox states of bistable rotaxanes.[3] We found that the mechanical motions of these mechanically interlocked molecules are influenced by their interactions with the surface and with neighboring molecules, as well as by the conformations of the dumbbell components.

RESULTS AND DISCUSSION

The rotaxane molecule ($\mathbf{R}^{4+}$), with disulfide groups attached to the stoppers on the dumbbell termini (Figure 1A), has been designed to bind at each end to Au{111}.

*Address correspondence to stoddart@northwestern.edu, psw@cnsi.ucla.edu.

Received for review March 16, 2010 and accepted May 25, 2010.

Published online June 11, 2010. 10.1021/nn100545r

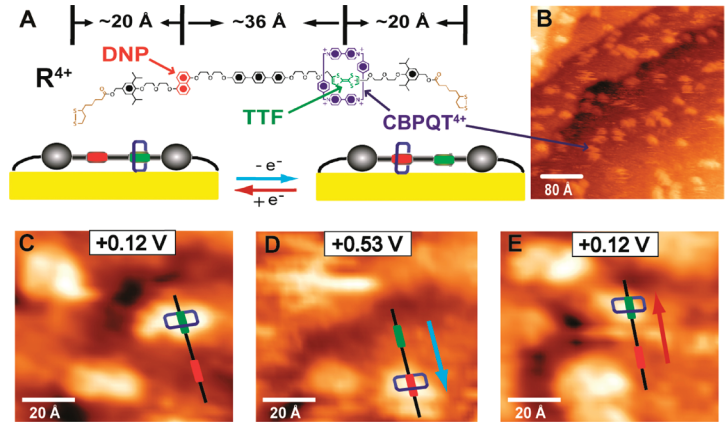

Figure 1. Structure and motion of a bistable rotaxane molecule, adsorbed on Au{111} investigated using electrochemical scanning tunneling microscopy. (A) The tetracationic cyclobis(paraquat-*p*-phenylene) ring ($CBPQT^{4+}$, blue) is known to move along the thread between two recognition sites (tetrathiafulvalene, TTF, green and 1,5-dioxynaphthalene, DNP, red stations) depending on the redox state of the TTF unit. (B) The protrusions are assigned as $CBPQT^{4+}$ rings. (C) In its reduced state at +0.12 V, the $CBPQT^{4+}$ ring prefers to encircle the TTF station. (D) Upon oxidation (+0.12 to +0.53 V) of the TTF station into a radical cation, electrostatic repulsion propels the ring to the DNP station (blue arrow). (E) Upon reduction (+0.53 to +0.12 V) of the TTF station to neutrality, the metastable state of the bistable rotaxane relaxes back to its thermodynamically favorable state, wherein the $CBPQT^{4+}$ ring occupies the TTF station (red arrow). Image conditions: V_{bias} = 0.3 V; $I_{tunneling}$ = 2 pA. The Faradaic current was typically less than 10 pA.

The sample is prepared with the desired coverage of 5−6 molecules/1000 Å^2 for STM imaging. The thread section of the dumbbell is assumed to assemble parallel to the surface.[11] The distance between the two stations (tetrathiafulalene, TTF, and 1,5-dioxynaphthalene, DNP) in the fully stretched dumbbell would be 36 Å. *In situ* STM images of the bistable rotaxane molecules attached to Au{111} showed (Figure 1B) apparent protrusions ~3 Å high and 10−12 Å laterally. No protrusions were observed when a bare gold surface and a control molecule, that is, the dumbbell compound without the tetracationic cyclobis(paraquat-*p*-phenylene) ($CBPQT^{4+}$) ring, were treated and imaged under identical conditions as for the bistable rotaxane (Supporting Information, Figure 2). The dumbbell component was apparently not sufficiently conductive to be resolved by STM. However, the $CBPQT^{4+}$ rings, having higher electrical conductivity and greater height relative to the dumbbell, appear as protrusions in STM images.[22] The protrusions are therefore assigned to be the $CBPQT^{4+}$ rings (Figure 1B), consistent with prior STM studies.[19]

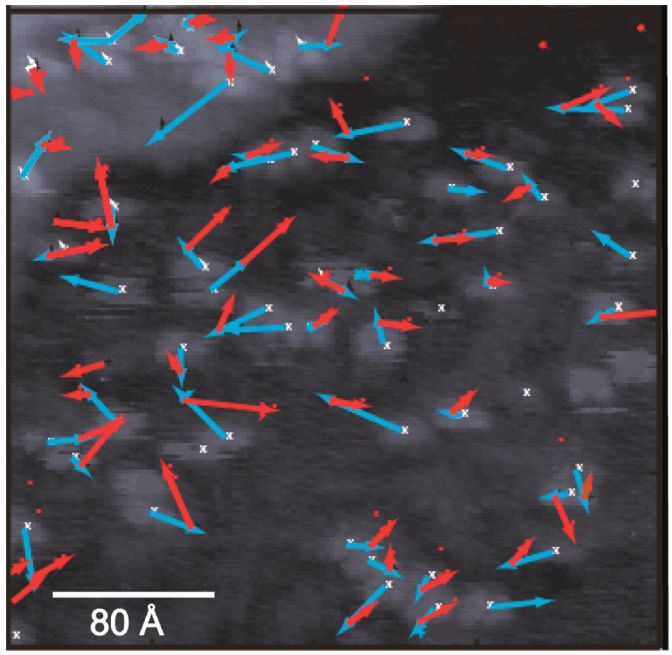

Figure 2. A STM image of R^{4+} adsorbed on Au{111} under 0.1 M $HClO_4$ solution. The three images with potentials +0.12, +0.53, and +0.12 V are superimposed and the protrusions on all three images have been marked. The trajectories of a large number of motions of $CBPQT^{4+}$ rings after potential steps from +0.12 to +0.53 V and back to +0.12 V are marked with blue and red lines, respectively, as in Figure 1C−E (320 Å × 320 Å).

To study the station changes in R^{4+}, we imaged the same surface region repeatedly and tracked the positions of protrusions using image processing routines, developed previously.[23−27] The images were corrected for lateral drift and the coordinates were identified by calculating the centroids of the protrusions. Trajectories were determined by minimizing sums of the squares of the displacements. We imaged the molecules at two different electrode potentials, +0.12 and +0.53 V, for which the TTF station is in the reduced (neutral) state, and in its oxidized (cationic) state, respectively (Supporting Information). Significant displacements were observed when the potential was stepped from +0.12 to +0.53 V (*vs* Ag/AgCl) and when the potential was returned to +0.12 V. Figure 1C,D shows the displacement trajectory (blue arrow) of one such ring. The correlations between the potential change and the $CBPQT^{4+}$ ring's motion suggest that when the TTF station becomes positively charged, it repels the $CBPQT^{4+}$ ring. Subsequently, the potential was stepped down from +0.53 to +0.12 V, and the protrusions underwent further displacements (Figure 1D,E; red arrow) suggesting that the $CBPQT^{4+}$ ring returns to its thermodynamically more favored positions encircling the neutral TTF

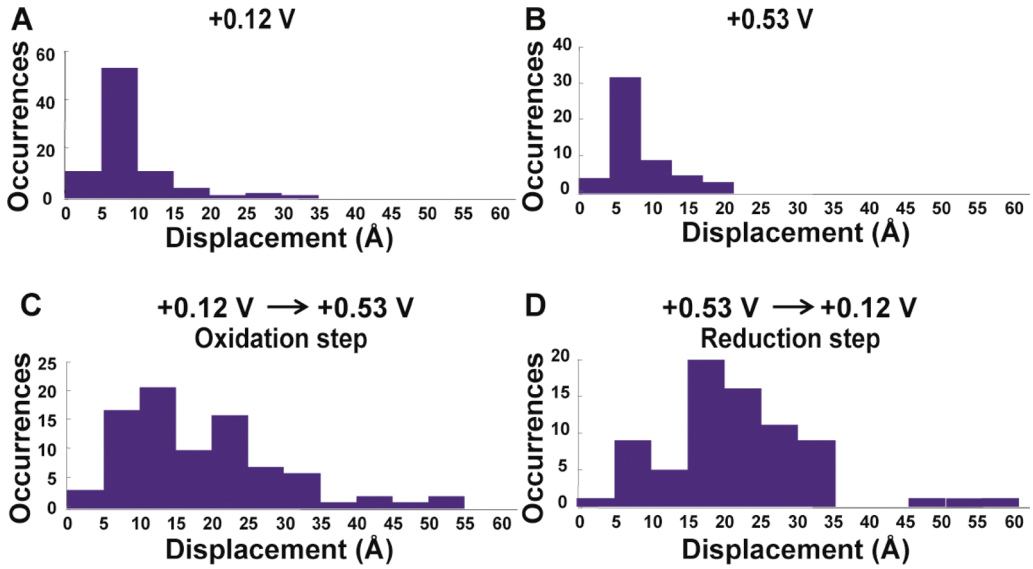

Figure 3. Histogram of measured displacements of protrusions over 10 min at different potentials: (A) the surface was equilibrated at +0.12 V; (B) the surface was equilibrated at +0.53 V; (C) the potential was stepped from +0.12 to +0.53 V and displacements were measured by comparing images acquired before and after the potential step; (D) the potential was stepped back from +0.53 to +0.12 V and again the displacements were measured.

station.[11] In this example (Figure 1C−E), shuttling of the ring between the two positions was ~30 Å, which corresponds to the approximate distance between the two stations in $\mathbf{R}^{4+}$. We observed many such motions, but the displacements varied, as described below.

Displacements of all the protrusions arising from the molecules in larger areas (320 × 320 Å^2) of the sample were tracked as station changing was induced by potential steps from +0.12 to +0.53 V and back (Figure 2, separated images are shown in Supporting Information, Figure S4). The images were superimposed and the protrusion centroids were filtered and correlated with the motions of each CBPQT^{4+} ring. The blue and red arrows represent displacements induced by these potential steps (as in Figure 1C−E). Figure 2 shows a wide range of displacements and angles between the trajectories during first (oxidation) and second (reduction) steps.

To understand the motions of CBPQT^{4+} rings of $\mathbf{R}^{4+}$ at different potentials, the displacements of a large number of protrusions were plotted in histograms (Figure 3). At each potential, the sample was equilibrated for 10 min. The root-mean-square (rms) displacements observed at +0.12 and +0.53 V were 5.5 and 6.2 Å (Figure 3A,B), respectively. Most of the protrusions remained at the same positions, within the measurement error (3−5 Å), when monitored in successive images under constant potential. A few protrusions (<10) appeared or disappeared between frames, despite appearing in the majority of images; we attribute this observation as most likely the result of conformational changes that reduce the conductance path through the rings to the substrate.[23,27] Here, the rms displacements of more than 90% of molecules are equal to or less than the distance between the two stations in the fully stretched model of $\mathbf{R}^{4+}$, and thus could be accounted for and attributed to the station changes.

Histograms of displacement correlated with oxidation steps (Figure 3C) showed a wide range of values (0−55 Å). The rms displacement was 20 Å, smaller than the distance between two recognition sites (36 Å) in a fully extended bistable rotaxane. Several factors influence the observed displacements. The wide distribution of values suggests the flexible nature of the dumbbell, along which the ring moves. The segment between the two stations (Figure 1A) is flexible because of the presence of the di(ethyleneglycol) chains, and thus, it is likely to deviate from a linear conformation. As a result of possible bending of the center segment between the TTF and DNP stations, the average displacement of the ring is expected to be smaller than 36 Å. In addition, conformational changes in the dumbbell and tethers would change the apparent ring displacement. A fully extended side segment is 20 Å long (Figure 1A), and a wagging of this segment around the thiolate tethers can shift the stations by up to 20 Å. Therefore, we anticipate the ring displacements to be 0−56 Å, consistent with the observed range. Conformational changes in the dumbbell component could be induced by the interplay of forces in which the electrochemically driven station changing competes with the π-electron interactions of one of the bipyridinium units in the CBPQT^{4+} with the substrate. The result of these forces could lead to conformational changes in the dumbbell and/or displacement of the thread section of the dumbbell. (If the dumbbell were fully stretched or was rigid by design, such conformational flexibility would not be possible.)

Displacements are relatively smaller where the molecules are clustered. Previously, ensemble studies

showed that the speed of switching was reduced dramatically when bistable rotaxanes were placed in condensed monolayers or gel matrices,[16] or on nanoparticles.[28] Nonetheless, adsorbed rotaxane molecules can block ion adsorption, and, in changing state, can lead to coordinated mechanical strain[12] as well as significant changes in optical properties if deliberately assembled on appropriate substrates.[29]

By stepping back the potential to +0.12 V (reduction step), a wide range of displacements was once again observed. The rms displacement of 16 Å is within the measurement error of the 20 Å displacement observed during the oxidation step. To understand the correlations between the two sets of motions, we calculated the angles between the trajectories during the first (oxidation) and second (reduction) steps. The angles of the second trajectories were measured, and it was found that 75% of the angles are between 90° and 270° (Supporting Information, Figure 3). By contrast, random walks would not display such anticorrelated directions. By controlling the oxidation state of the TTF units, the $CBPQT^{4+}$ rings on individual molecules can be driven back and forth between the stations. Although STM has not directly visualized the stations on the dumbbells, the reversibility provides evidence that electrochemical input is driving the motion of the rings between stations. Because of the flexibility of the dumbbells, one does not expect most of the $CBPQT^{4+}$ rings to move back and forth between fixed positions.

CONCLUSIONS AND OUTLOOK

Using ECSTM, we observed electrochemically controlled station changes of individual bistable rotaxane molecules *in situ*. Motions of the $CBPQT^{4+}$ rings were correlated with redox states of the TTF station and displayed partial reversibility. The trajectories of the rings suggest that once a bistable rotaxane molecule is adsorbed on a surface, the motion of the $CBPQT^{4+}$ ring relative to the dumbbell is affected by its local environment and the flexibility of the molecule. Bistable rotaxane molecules with *rigid* dumbbells should enable consistent and fully reversible motions, as well as direct visualization of the rings *and* the shafts of the molecules. The molecular design and synthesis of such systems are underway. Consistent and complete reversibility of switching in these bistable molecules will be required for efficient actuation of nanoelectromechanical devices[12] and for reliable nanoelectronic device applications.[8]

MATERIALS AND METHODS

Synthesis of Rotaxane Molecule and Control Molecule. The rotaxane molecule ($\mathbf{R}^{4+}$), with disulfide groups attached to the stoppers on the dumbbell termini (Figure 1A), has been designed to bind at each end to Au{111}. Details of the synthesis of $\mathbf{R}^{4+}$ and control molecule **8** have been provided in the Supporting Information.

Preparation of Rotaxane Monolayer on Substrate. After cleaning a Au{111} single crystal disk with piranha solution (3:1 mixture of H_2SO_4 and H_2O_2) (Note: Dangerous! Acidic and highly corrosive), the Au{111} disk was hydrogen flame annealed and cooled under argon before being immersed in the $\mathbf{R} \cdot 4PF_6$ solution (~10 μM). Only a 10−20 s immersion was done to achieve the desired coverage (5−6 molecules/1000 $Å^2$) for STM imaging. The sample was rinsed with acetonitrile, nitrogen dried, and then transferred to the STM electrochemical cell with 0.1 M $HClO_4$ solution.

Electrochemical Scanning Tunneling Microscopy. A PicoSPM microscope (Molecular Imaging, AZ) controlled by an RHK STM-100 controller (RHK Technology, Troy, MI) and electrochemically etched tungsten tips insulated with paraffin wax were used to image the samples. The electrode potentials given are in reference to a Ag/AgCl electrode, although a platinum wire was used as a quasi-reference electrode.

Acknowledgment. Support from the NSF-supported Center for Nanoscale Science (a MRSEC), the Department of Energy (Grant No. DE-FG02-07ER15877), the Center on Functional Engineered and NanoArchitectonics (FENA, sponsored by the Semiconductor Research Corporation), and the Kavli Foundation are gratefully acknowledged. We thank Prof. Kevin Kelly and Mr. Bala Pathem for helpful discussions.

Supporting Information Available: Additional experimental data on the synthesis of $\mathbf{R}^{4+}$ and control molecule **8** are provided in details. The details of cyclic voltametry of adsorbed $\mathbf{R}^{4+}$ is discussed. This material is available free of charge *via* the Internet at http://pubs.acs.org.

REFERENCES AND NOTES

1. Amabilino, D. B.; Stoddart, J. F. Interlocked and Intertwined Structures and Superstructures. *Chem. Rev.* **1995**, *95*, 2725–2828.
2. Badjic, J. D.; Balzani, V.; Credi, A.; Silvi, S.; Stoddart, J. F. A Molecular Elevator. *Science* **2004**, *303*, 1845–1849.
3. Balzani, V.; Gomez-Lopez, M.; Stoddart, J. F. Molecular Machines. *Acc. Chem. Res.* **1998**, *31*, 405–414.
4. Kay, E. R.; Leigh, D. A.; Zerbetto, F. Synthetic Molecular Motors and Mechanical Machines. *Angew. Chem., Int. Ed.* **2007**, *46*, 72–191.
5. Kottas, G. S.; Clarke, L. I.; Horinek, D.; Michl, J. Artificial Molecular Rotors. *Chem. Rev.* **2005**, *105*, 1281–1376.
6. Michl, J.; Sykes, E. C. H. Molecular Rotors and Motors: Recent Advances and Future Challenges. *ACS Nano* **2009**, *3*, 1042–1048.
7. Stoddart, J. F. The Master of Chemical Topology (Jean-Pierre Sauvage). *Chem. Soc. Rev.* **2009**, *38*, 1521–1529.
8. Green, J. E.; Choi, J. W.; Boukai, A.; Bunimovich, Y.; Johnston-Halperin, E.; Delonno, E.; Luo, Y.; Sheriff, B. A.; Xu, K.; Shin, Y. S.; *et al.* A 160-Kilobit Molecular Electronic Memory Patterned at 10(11) Bits per Square Centimeter. *Nature* **2007**, *445*, 414–417.
9. Ikeda, T.; Saha, S.; Aprahamian, I.; Leung, K. C. F.; Williams, A.; Deng, W. Q.; Flood, A. H.; Goddard, W. A.; Stoddart, J. F. Toward Electrochemically Controllable Tristable Three-Station [2]Catenanes. *Chem., Asian J.* **2007**, *2*, 76–93.
10. Li, D. B.; Paxton, W. F.; Baughman, R. H.; Huang, T. J.; Stoddart, J. F.; Weiss, P. S. Molecular, Supramolecular, and Macromolecular Motors and Artificial Muscles. *MRS Bull.* **2009**, *34*, 671–681.
11. Liu, Y.; Flood, A. H.; Bonvallett, P. A.; Vignon, S. A.; Northrop, B. H.; Tseng, H. R.; Jeppesen, J. O.; Huang, T. J.;

Brough, B.; Baller, M.; *et al.* Linear Artificial Molecular Muscles. *J. Am. Chem. Soc.* **2005**, *127*, 9745–9759.
12. Juluri, B. K.; Kumar, A. S.; Liu, Y.; Ye, T.; Yang, Y.-W.; Flood, A. H.; Fang, L.; Stoddart, J. F.; Weiss, P. S.; Huang, T. J. A Mechanical Actuator Driven Electrochemically by Artificial Molecular Muscles. *ACS Nano* **2009**, *3*, 291.
13. Brouwer, A. M.; Frochot, C.; Gatti, F. G.; Leigh, D. A.; Mottier, L.; Paolucci, F.; Roffia, S.; Wurpel, G. W. H. Photoinduction of Fast, Reversible Translational Motion in a Hydrogen-Bonded Molecular Shuttle. *Science* **2001**, *291*, 2124–2128.
14. Collin, J. P.; Dietrich-Buchecker, C.; Gavina, P.; Jimenez-Molero, M. C.; Sauvage, J. P. Shuttles and Muscles: Linear Molecular Machines Based on Transition Metals. *Acc. Chem. Res.* **2001**, *34*, 477–487.
15. Anelli, P.-L.; Spencer, N.; Stoddart, J. F. A Molecular Shuttle. *J. Am. Chem. Soc.* **1991**, *113*, 5131–5133.
16. Choi, J. W.; Flood, A. H.; Steuerman, D. W.; Nygaard, S.; Braunschweig, A. B.; Moonen, N. N. P.; Laursen, B. W.; Luo, Y.; Delonno, E.; Peters, A. J.; *et al.* Ground-State Equilibrium Thermodynamics and Switching Kinetics of Bistable [2]Rotaxanes Switched in Solution, Polymer Gels, and Molecular Electronic Devices. *Chem.—Eur. J.* **2006**, *12*, 261–279.
17. Tseng, H. R.; Wu, D. M.; Fang, N. X. L.; Zhang, X.; Stoddart, J. F. The Metastability of an Electrochemically Controlled Nanoscale Machine on Gold Surfaces. *ChemPhysChem* **2004**, *5*, 111–116.
18. Feng, M.; Gao, L.; Du, S. X.; Deng, Z. T.; Cheng, Z. H.; Ji, W.; Zhang, D. Q.; Guo, X. F.; Lin, X.; Chi, L. F.; *et al.* Observation of Structural and Conductance Transition of Rotaxane Molecules at a Submolecular Scale. *Adv. Funct. Mater.* **2007**, *17*, 770–776.
19. Shigekawa, H.; Miyake, K.; Sumaoka, J.; Harada, A.; Komiyama, M. The Molecular Abacus: STM Manipulation of Cyclodextrin Necklace. *J. Am. Chem. Soc.* **2000**, *122*, 5411–5412.
20. He, Y.; Ye, T.; Borguet, E. Porphyrin Self-Assembly at Electrochemical Interfaces: Role of Potential Modulated Surface Mobility. *J. Am. Chem. Soc.* **2002**, *124*, 11964–11970.
21. Ye, T.; He, Y. F.; Borguet, E. Adsorption and Electrochemical Activity: An *in Situ* Electrochemical Scanning Tunneling Microscopy Study of Electrode Reactions and Potential-Induced Adsorption of Porphyrins. *J. Phys. Chem. B* **2006**, *110*, 6141–6147.
22. Bumm, L. A.; Arnold, J. J.; Cygan, M. T.; Dunbar, T. D.; Burgin, T. P.; Jones, L.; Allara, D. L.; Tour, J. M.; Weiss, P. S. Are Single Molecular Wires Conducting. *Science* **1996**, *271*, 1705–1707.
23. Donhauser, Z. J.; Mantooth, B. A.; Kelly, K. F.; Bumm, L. A.; Monnell, J. D.; Stapleton, J. J.; Price, D. W.; Rawlett, A. M.; Allara, D. L.; Tour, J. M.; *et al.* Conductance Switching in Single Molecules through Conformational Changes. *Science* **2001**, *292*, 2303–2307.
24. Mantooth, B. A.; Donhauser, Z. J.; Kelly, K. F.; Weiss, P. S. Cross-Correlation Image Tracking for Drift Correction and Adsorbate Analysis. *Rev. Sci. Instrum.* **2002**, *73*, 313–317.
25. Moore, A. M.; Mantooth, B. A.; Donhauser, Z. J.; Maya, F.; Price, D. W.; Yao, Y. X.; Tour, J. M.; Weiss, P. S. Cross-Step Place-Exchange of Oligo(phenylene−ethynylene) Molecules. *Nano Lett.* **2005**, *5*, 2292–2297.
26. Mantooth, B. A.; Sykes, E. C. H.; Han, P.; Moore, A. M.; Donhauser, Z. J.; Crespi, V. H.; Weiss, P. S. Analyzing the Motion of Benzene on Au{111}: Single Molecule Statistics from Scanning Probe Images. *J. Phys. Chem. C* **2007**, *111*, 6167–6182.
27. Weiss, P. S. Functional Molecules and Assemblies in Controlled Environments: Formation and Measurements. *Acc. Chem. Res.* **2008**, *41*, 1772–1781.
28. Coskun, A.; Wesson, P. J.; Klajn, R.; Trabolsi, A.; Fang, L.; Olson, M. A.; Dey, S. K.; Grzybowski, B. A.; Stoddart, J. F. Molecular-Mechanical Switching at the Nanoparticle-Solvent Interface: Practice and Theory. *J. Am. Chem. Soc.* **2010**, *132*, 4310–4320.
29. Zheng, Y. B.; Yang, Y. W.; Jensen, L.; Fang, L.; Juluri, B. K.; Flood, A. H.; Weiss, P. S.; Stoddart, J. F.; Huang, T. J. Active Molecular Plasmonics: Controlling Plasmon Resonances with Molecular Switches. *Nano Lett.* **2009**, *9*, 819–825.